# Novel Cardiac Computed Tomography Methods for the Assessment of Anthracycline Induced Cardiotoxicity

Attila Feher[1]*, Lauren A. Baldassarre[1,2] and Albert J. Sinusas[1,2,3]

[1] Department of Internal Medicine, Section of Cardiovascular Medicine, Yale University School of Medicine, New Haven, CT, United States, [2] Department of Radiology and Biomedical Imaging, Yale University School of Medicine, New Haven, CT, United States, [3] Department of Biomedical Engineering, Yale University, New Haven, CT, United States

Anthracyclines are among the most frequently utilized anti-cancer therapies; however, their use is frequently associated with off-target cardiotoxic effects. Cardiac computed tomography (CCT) is a validated and rapidly evolving technology for the evaluation of cardiac structures, coronary anatomy and plaque, cardiac function and preprocedural planning. However, with emerging new techniques, CCT is rapidly evolving to offer information beyond the evaluation of cardiac structure and epicardial coronary arteries to provide details on myocardial deformation, extracellular volume, and coronary vasoreactivity. The potential for molecular imaging in CCT is also growing. In the current manuscript we review these emerging computed tomography techniques and their potential role in the evaluation of anthracycline-induced cardiotoxicity.

Keywords: computed tomography, anthracycline, doxorubicin, cardiotoxicity, cardiooncology, cardiovascular computed tomography, strain, fibrosis

## INTRODUCTION

Cancer is the second leading cause of death in the United States. Approximately 1.9 million new cancer cases and 600,000 cancer deaths are projected to occur in the United States in 2021 (1). As of 2019, there were an estimated 16.9 million cancer survivors living in the United States and this number is projected to increase to 22.2 million by 2030 (2). In view of the significant improvement in survival, cardiovascular health has become an emerging focus of interest in cancer survivals.

Anthracyclines are among the most frequently utilized anti-cancer agents and they rank high among the most effective antineoplastic therapies (3). The first anthracycline, daunorubicin was discovered in the early 1960s by Di Marco et al. who isolated daunorubicin from a strain of *Streptomyces peucetius* (4). Shortly, this was followed by the discovery of other anthracycline agents which all demonstrated anti-cancer properties, including the most frequently used anthracyclines in addition to daunorubicin: doxorubicin, idarubicin, epirubicin and mitoxantron. The exact mechanism of anthracycline effect on cancer cells remains unclear, however it is likely multifactorial. The following mechanisms have been suggested (1) intercalation into deoxyribonucleic acid (DNA), leading to inhibited protein synthesis; (2) free radical generation leading to inflammation, lipid peroxidation, and DNA damage; (3) DNA binding, alkylation or cross-linking and/or interference with DNA unwinding or DNA strand separation and helicase activity; (4) direct membrane and other cellular cytotoxic effects; and (5) topoisomerase II inhibition leading to DNA damage and apoptosis (3). Despite the fact that it has been almost 60 years since the discovery of anthracyclines, and despite the recent unprecedented

breakthrough in cancer treatment achieved by targeted oncologic therapies, about 30% of breast cancer patients, 50 to 70% of elderly lymphoma patients, and up to 50 to 60% of childhood cancer patients are treated with an anthracycline based regimen (5).

Cardiac computed tomography (CCT) is a validated, rapidly evolving technology for the evaluation of cardiac structures with or without contrast administration, including evaluation of coronary anatomy and coronary atherosclerotic disease with high spatial resolution, evaluation of cardiac function and preprocedural planning for electrophysiologic and percutaneous valvular interventions. This review aims to summarize the current and future CCT applications that could be used for pre-treatment risk evaluation, cardiotoxicity surveillance and early identification during anthracycline therapy (**Figure 1**). Although CCT has value for the evaluation of cancer therapy associated valvular heart disease, pericardial disease and primary/secondary malignancies involving the heart, discussion of these applications is beyond the scope of this review.

## MECHANISM OF ANTHRACYCLINE INDUCED CARDIOTOXICITY

Anthracyclines have become one of the most effective antineoplastic agents, however, it was recognized relatively early that their use is associated with increasing incidence of heart failure (6, 7). Importantly, one of these early studies demonstrated the dose dependent association between the most commonly used anthracycline, doxorubicin, and cardiotoxicity, namely that the incidence of clinical heart failure was exponentially higher in patients who were exposed to doxorubicin over a cumulative dose of 550 mg/m$^2$ (7). This has been confirmed by a later retrospective pooled cohort study showing that the incidence of heart failure varies with exposed cumulative dose of anthracyclines: 4.7% at 400 mg/m$^2$, 26% at 550 mg/m$^2$ and 48% at 700 mg/m$^2$ (8). Importantly, the incidence of anthracycline induced cardiotoxicity (AIC) is influenced by many other factors including genetic variability, age (with children and the elderly at higher risk), previous treatment with cardiotoxic drugs or radiation therapy, and history of cardiovascular disease (9).

The mechanisms responsible for AIC are complex and incompletely understood. Initial observations linked doxorubicin induced cardiotoxicity to the formation of reactive oxygen species (ROS) leading to myocyte damage by oxidative injury (10–13). Myocardial injury by complex formation of anthracyclines with topoisomerase IIb causing double-stranded DNA breaks has been more recently proposed as an alternative main mechanism for AIC (5).

Cardiomyocytes comprise 80% of the cardiac mass, however they only account for less than 20% of the cardiac cells. Other cells, such as endothelial cells, smooth muscle cells, fibroblasts and adipocytes provide structural and functional support and form a unique environment for the cardiomyocytes. Emerging evidence suggests that the deleterious effect of anthracyclines is not limited to cardiomyocytes. As such, anthracycline

administration has been linked to microvascular injury by direct endothelial DNA damage (14), by promoting apoptosis through oxidative stress, (15, 16) or by interfering with endothelial nitric oxide bioavailability and nitric oxide signaling (17). Related to this, in rodent models, AIC could be rescued by targeting endothelial inflammation or angiogenesis (18, 19). A recent review concluded that the microvascular endothelium serves an important novel target for the early detection, prevention, and treatment of AIC (20).
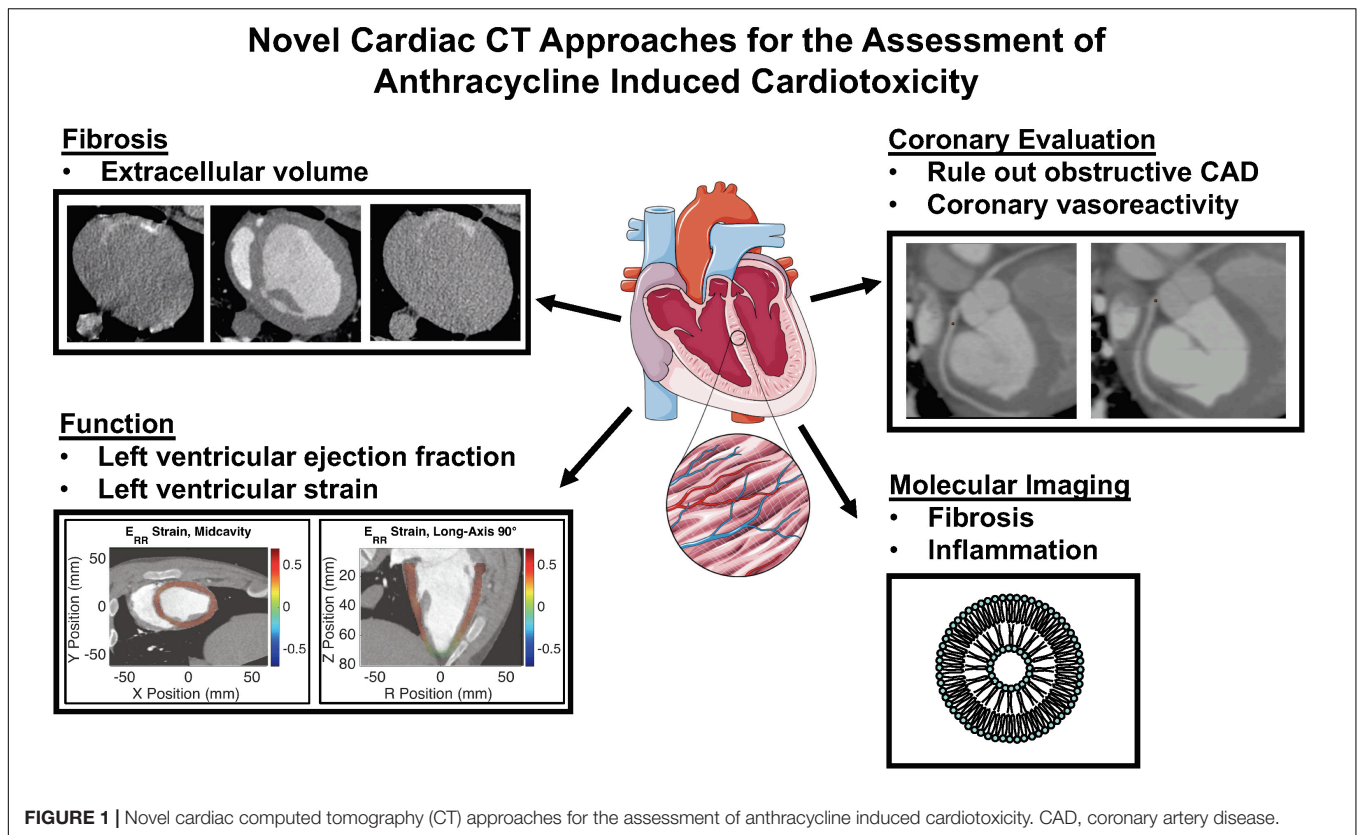
The extracellular matrix plays a unique role in cardiac homeostasis, not only by providing structural support, but also by facilitating force transmission and cell to cell communication. Although there are multiple pathways that contribute to anthracycline induced cardiac injury, ultimately all these processes lead to a common downstream pathway that results in alteration of proteolytic pathways leading to disruption in the very fine balance of myocardial matrix metalloproteinases and their inhibitors resulting in deposition of components of the extracellular matrix and tissue fibrosis (21–23).

## EVALUATION OF LEFT VENTRICULAR SYSTOLIC FUNCTION AND STRAIN: ROLE OF CT IN ASSESSMENT OF ANTHRACYCLINE INDUCED CARDIOTOXICITY

Multi-phase cardiac computed tomography (CT) with retrospective ECG gating allows for 3-dimensional analysis of the cardiac function with high spatial resolution. Advances in CT technology have resulted in lower radiation dose and higher temporal resolution for cardiac imaging techniques (24). Electrocardiogram pulsing reduces radiation by modulating the tube current during the scan, applying higher amount of tube current during diastole with lower tube current during the rest of the cardiac cycle (25).

Computed tomography based evaluation of left ventricular volumes has been reported as early as 2004, (26); however, the routine use of CT for left ventricular systolic function evaluation has been limited due to the elevated radiation dose associated with retrospectively gated studies.

Left ventricular global longitudinal strain (GLS) as assessed by 2-dimensional transthoracic echocardiography is a well described early predictor of AIC (27, 28). LV GLS is a more sensitive, reproducible measure of LV dysfunction when compared to LVEF. In a recent meta-analysis, measurement of echocardiographic GLS after initiation of anthracycline based chemotherapy with or without trastuzumab had good prognostic performance for predicting subsequent cancer therapy-related cardiac dysfunction defined as clinically significant change in left ventricular ejection fraction (LVEF) with or without new-onset heart failure symptoms (27). The recently published SUCCOR (Strain sUrveillance of Chemotherapy for improving Cardiovascular Outcomes) international multicenter prospective randomized controlled trial evaluated whether echocardiographic GLS guided cardioprotective therapy would

**FIGURE 1 |** Novel cardiac computed tomography (CT) approaches for the assessment of anthracycline induced cardiotoxicity. CAD, coronary artery disease.

prevent reduction in LVEF and development of chemotherapy induced cardiotoxicity in comparison to standard, LVEF guided care in a high risk population receiving cardiotoxic chemotherapy (29). Despite the fact that the primary outcome, defined as change in LVEF was not significantly different between the 2 arms at 1 year follow-up, in the GLS-guided group fewer patients met the prespecified criteria for chemotherapy induced cardiotoxicity compared to the LVEF-guided group. The LVEF at 1 year follow-up approached achieved a significant difference for the LVEF-guided versus the GLS-guided groups (55 ± 7% versus 57 ± 6%, $p = 0.05$) (29). In this trial, restricting the analysis to cancer patients who received cardioprotective therapy, the LVEF-guided arm had significantly more reduction in LVEF on follow-up echocardiogram when compared to GLS-guided arm (9 ± 11% vs. 3 ± 7%, $p = 0.03$).

The possibility of quantitative assessment of regional myocardial deformation from cine CT was demonstrated by Shi et al. using shape-based tracking of the ventricular surface (30) and has been subsequently reported and validated by several other groups (31, 32). Tissue tracking is used to calculate strain between sequential image frames, from systole to diastole, by using techniques adapted from echocardiography and cardiac MRI (30). The feasibility of performing CT strain has been demonstrated in large animal studies (**Figure 2**) (33) and in humans (34–37). A recent study assessing 44 heart failure patients undergoing both ECG gated cardiac CT and cardiac MRI within 24 h, showed good reproducibility of CT strain measurements and detected a good correlation between CT

global longitudinal strain (GLS) and MRI GLS (38). In patients undergoing transcatheter aortic valve replacement CT strain was predictive of adverse outcomes, (36) and improvement in CT derived global longitudinal and principal strain has been demonstrated after transcatheter aortic valve replacement (34). The optimal evaluation of regional strain from CT images should employ 3-dimensional tracking of regional myocardial displacements (37), and probably will employ deep learning (39). Automated segmentation of left ventricular cavity in temporal cardiac image sequences (consisting of multiple time-points) is a fundamental requirement for quantitative analysis of cardiac structural and functional changes. A recently published approach employed a spatial-sequential network with bi-directional learning of 4D CT images which out-performed existing approaches for automated LV segmentation (40). Currently, there are commercially available programs for calculation of regional myocardial strain from contrast cine CT but these are based on 2D analysis of stacks of images (41). Although CT imaging holds promise for true high-resolution 3D analysis of regional myocardial strain, to date CT derived strain has not yet been assessed as a tool for the early prediction of AIC.

## CT EVALUATION OF EPICARDIAL AND MICROVASCULAR CORONARY INJURY

Cardiac CT plays a central role in the evaluation of coronary artery disease (CAD) in patients presenting with chest pain
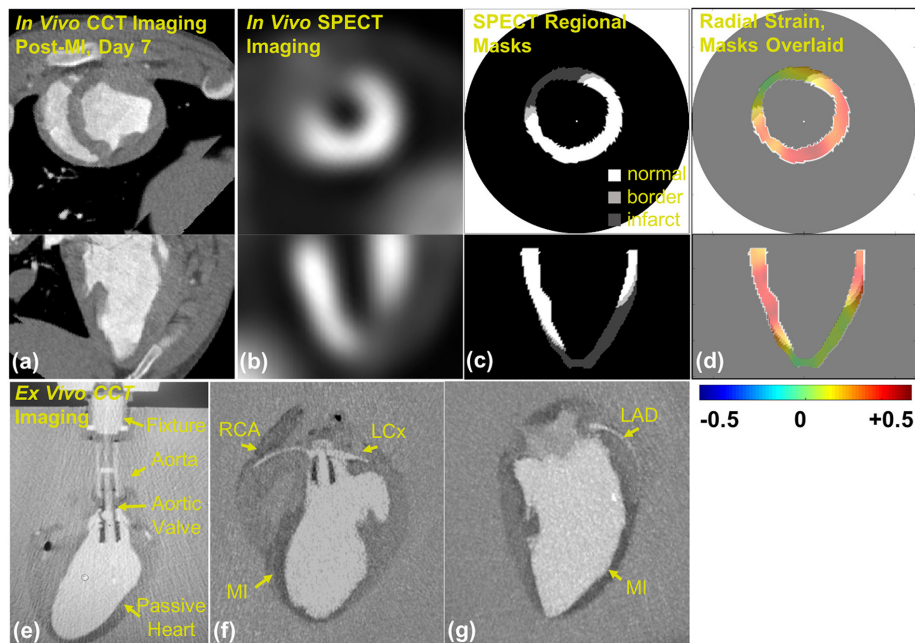
**FIGURE 2 |** Contrast CineCT and 99mTc-Tetrofosmin SPECT imaging and masking in porcine heart: (a) *in vivo* contrast CineCT short- and long-axis imaging of porcine heart on day 7 after myocardial infarction (MI), (b) *in vivo* SPECT short- and long-axis imaging of the porcine heart on day 7 after MI, (c) SPECT-derived regional masks for strain fields of normal (white, > 60% max intensity), border (light gray, > 50% and < 60% max intensity), and infarct (dark gray, < 50% max intensity) regions, and (d) SPECT strain masks overlaid on radial strain field. *Ex vivo* contrast CineCT imaging of the arrested porcine heart 7 after hydrogel delivery: (e) custom aortic valve insert and suspension fixture, (f) MI region and perfusion of right coronary artery (RCA) and left circumflex coronary artery (LCx), and (g) MI region and left anterior descending coronary artery (LAD). Note: this image is reproduced with permission from Midgett et al. (33).

syndromes. The recent chest pain guideline specifies the use of coronary CT angiography (CTA) as a Class I recommendation for the exclusion of atherosclerotic plaque and obstructive CAD in intermediate-risk patients with acute chest pain and no known CAD (42). Coronary CT angiography also meets Class I recommendation for diagnosis of CAD, risk stratification and guiding treatment decisions for patients with stable chest pain who have an intermediate to high risk of obstructive CAD. Pre-existing CAD is known to increase the risk of development of cardiovascular complications in patients receiving anthracycline-based chemotherapy or receiving chest irradiation as a part of anti-cancer therapy (43), however current guidelines do not recommend routine assessment for evidence of CAD prior to initiation of anthracycline based chemotherapy. On the other hand, heart failure guidelines recommend the exclusion of CAD in patients with a new diagnosis of heart failure with reduced ejection fraction (44). Coronary CTA has been demonstrated to be a highly sensitive tool for the detection of obstructive CAD in patients with dilated cardiomyopathy (45, 46). Therefore, coronary CTA might be utilized to exclude epicardial coronary stenosis in patients with prior anthracycline exposure and newly developed reduced left ventricular ejection fraction. In a single center retrospective study, coronary CTA findings altered the therapeutic plan in 52% of 80 cancer patients undergoing coronary CTA by aiding in the decision of withholding, altering or continuing oncologic therapy (47). Coronary CTA can be used to rule out obstructive CAD in

cancer patients with increased troponin levels after undergoing anthracycline treatment, which can be observed in up to 30% of patients receiving high dose chemotherapy (48). In addition, coronary CTA can be particularly helpful with the initial evaluation of patients presenting with chest pain and concurrent severe thrombocytopenia (relatively common side effect of anthracyclines), when invasive evaluation is often not feasible with relative contraindication for the use of heparin containing products. In addition, CT angiography can be further utilized for the evaluation of venous and arterial thrombosis, which are emerging new contributors to the development of AIC (49).

Coronary artery calcium (CAC) scoring by non-contrast CT provides a marker of CAD burden within the epicardial coronary arteries (50). The presence of CAC is a strong predictor of future cardiovascular risk with higher prognostic value than traditional risk assessment tools such as the Framingham risk score and the Atherosclerotic Cardiovascular Disease (ASCVD) risk score (50, 51). Moreover, CAC quantification has been demonstrated to be feasible on non-gated, non-cardiac chest CT scans with excellent correlation with standard CAC score derived from gated cardiac acquisitions (52). El-Sabbagh et al. demonstrated an average increase of 35% in non-gated CAC score in 112 lymphoma patients undergoing chemotherapy when comparing CAC score on pre and post chemotherapy non-gated CT examinations (53). Automated CAC scoring on non-gated non-contrast CT scans could be used as a fast and low-cost tool to identify cancer patients at higher cardiovascular

risk, allowing implementation of cardiovascular risk reduction strategies prior to initiation of anthracycline based therapy. Importantly, the recently published joint guidelines the Society of Cardiovascular Computed Tomography and the Society of Thoracic Radiology recommends visual estimation for presence of CAC and encourages computation of a non-gated CAC score for all non-contrast chest CT examinations (54).

Recently, our group has developed a novel CT based strategy for the evaluation of coronary microvascular dysfunction associated with AIC (28). In this study, we used a canine model of doxorubicin-induced cardiotoxicity, where canines received weekly intravenous doxorubicin (1 mg/kg) for 12–15 weeks resulting in significant reduction in the left ventricular ejection fraction and histological evidence of cardiotoxicity by the end of therapy. Epicardial coronary artery diameters were measured at pre-specified distances from vessel origins from coronary CTA performed during rest, and in the presence of adenosine and dobutamine stress. Adenosine vasodilator responses (increase in epicardial coronary diameter) were impaired after ∼4 mg/kg and ∼8 mg/kg cumulative doxorubicin dosing, whereas dobutamine induced dilation response was preserved at ∼4 mg/kg, but tended to decrease at ∼8 mg/kg of doxorubicin (**Figure 3**). A significant LVEF reduction was observed only at 12–15 mg/kg doxorubicin dosing. These findings suggest an early impairment in microvascular responses in AIC. Adenosine-induced epicardial coronary responses depend on a direct vasodilatory effect on vascular smooth muscle and on subsequent flow-mediated shear stress endothelial dependent vasodilation due to local endothelial nitric oxide secretion. In contrast, dobutamine-induced vasodilation is mostly a result of direct stimulation of myocardial and vascular β-adrenergic receptors. Our results may indicate the susceptibility of the endothelium to anthracyclines leading to an early impairment in endothelium-dependent coronary vasodilation.

## CT EVALUATION OF EXTRACELLULAR VOLUME IN ANTHRACYCLINE-INDUCED CARDIOTOXICITY

Assessment and quantification of myocardial late gadolinium enhancement (LGE) using magnetic resonance imaging (MRI) has been well validated for quantitative evaluation of focal myocardial fibrosis in the setting of myocardial infarction and non-ischemic cardiomyopathy (55–58). With cardiac MRI the extracellular volume (ECV) of the myocardium can be estimated by measuring both blood and myocardial longitudinal (T1) relaxation times pre and post gadolinium administration, using the following formula:

$$ECV\ MRI = (1 - hematocrit)\frac{\frac{1}{T1\ myo\ post} - \frac{1}{T1\ myo\ pre}}{\frac{1}{T1\ blood\ post} - \frac{1}{T1\ blood\ pre}}$$

where, T1 myo and T1 blood represent the myocardial and blood T1 values before (pre) and after (post) gadolinium contrast administration. Several studies reported on excellent correlation between myocardial ECV assessed by MRI and quantitative
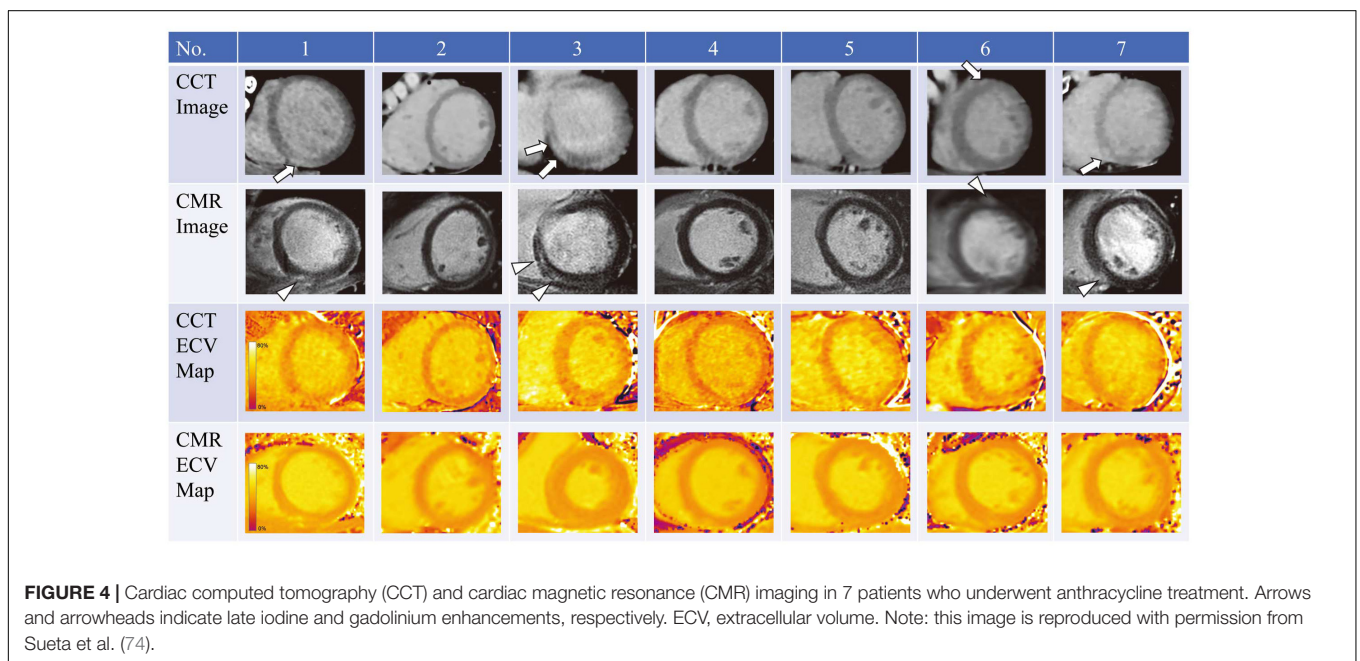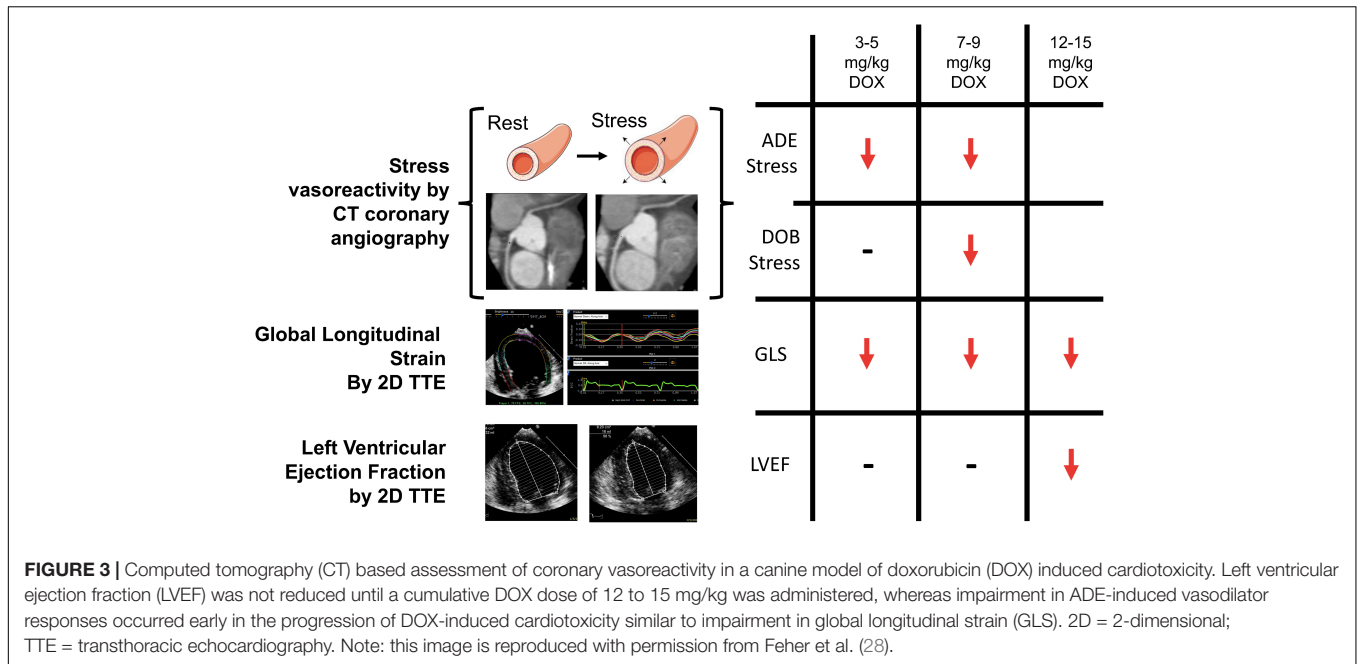
histopathology (59–61). Importantly, multiple MRI studies have demonstrated that the ECV was elevated in patients treated with anthracyclines compared to matched control populations (62–64). Based on the observed association between increased ECV and decrease in intracellular water lifetime (a marker of cardiomyocyte size) and LV mass in response to anthracycline based chemotherapy, one of these studies suggested that in anthracycline-induced cardiac injury the increase in ECV may be due to a decrease in LV mass from cardiomyocyte loss rather than interstitial fibrosis and edema (64). This hypothesis will require further investigation. MRI has been invaluable for the evaluation of changes in ECV in AIC; however, there are minor drawbacks with the use of MRI for the evaluation of ECV, including: (1) prolonged examination protocols especially with the need of pre and post contrast T1 mapping, (2) associated increased medical cost, and (3) inability to image patients with claustrophobia.

In the last decade, CT has emerged as an additional tool for the assessment of cardiac fibrosis. The evaluation of ECV by CT relies upon the same principle as assessment with MRI. The CT imaging protocol requires acquisition of a low dose ECG-gated cardiac CT prior to contrast administration and repeat imaging following administration of contrast at a delayed timepoint, usually 10 min after iodinated contrast administration (65). The CT derived estimate of ECV is obtained using the following formula:

$$ECV\ CT = (1 - hematocrit)\frac{\Delta\ HU\ myo}{\Delta\ HU\ blood}$$

where, Δ HU myo and Δ HU blood are the change in Hounsfield unit attenuation pre- and post-contrast administration (e.g., HU post-contrast – HU pre-contrast) in the myocardium and the blood, respectively. ECV estimated by CT has been shown to correlate well with both MRI derived ECV (65–67) and pathological indices of fibrosis (66). Moreover CT derived ECV has been shown to be prognostic of adverse cardiovascular events in aortic stenosis in patients undergoing periprocedural CT evaluation (68).

A handful of studies have investigated the use of ECV CT index in the assessment of AIC (69–74). Zhou et al. compared ECV assessed by CT and MRI in a chronic canine model of AIC (70). In this study canines were administered intravenous doxorubicin every 3 weeks achieving a cumulative dose of 240 mg/m² and had follow-up CT and MRI examination at 16 and 24 weeks. CT detected an increase in ECV over time following doxorubicin administration (baseline: 25.2%, 16 weeks: 34.4%, 24 weeks: 37.7%). In this study ECV CT correlated well with both MRI ECV and with indices of fibrosis on histological analysis. In addition to animal models of AIC, a few studies have also looked at CT derived ECV in cancer patients receiving anthracycline-based chemotherapy regimens (71–74). In a small study, Sueta et al. found the ECV CT (33.0 ± 2.5%) elevated in 7 cancer patients with documented AIC which was confirmed by CMR assessment of ECV (**Figure 4**) (74). Another study evaluated 44 patients who previously received anthracycline based chemotherapy regimens, and found significantly higher ECV CT index in the patients with documented AIC (n = 7, ECV: 30.3 ± 4.8%) versus patients who received anthracycline without

**FIGURE 3 |** Computed tomography (CT) based assessment of coronary vasoreactivity in a canine model of doxorubicin (DOX) induced cardiotoxicity. Left ventricular ejection fraction (LVEF) was not reduced until a cumulative DOX dose of 12 to 15 mg/kg was administered, whereas impairment in ADE-induced vasodilator responses occurred early in the progression of DOX-induced cardiotoxicity similar to impairment in global longitudinal strain (GLS). 2D = 2-dimensional; TTE = transthoracic echocardiography. Note: this image is reproduced with permission from Feher et al. (28).



**FIGURE 4 |** Cardiac computed tomography (CCT) and cardiac magnetic resonance (CMR) imaging in 7 patients who underwent anthracycline treatment. Arrows and arrowheads indicate late iodine and gadolinium enhancements, respectively. ECV, extracellular volume. Note: this image is reproduced with permission from Sueta et al. (74).

cardiac dysfunction (*n* = 37, ECV: 27.5 ± 3.1%) or control patients who did not receive cardiotoxic chemotherapy (*n* = 20, ECV: 26.2 ± 2.5%) (73). Monti et al. performed a retrospective study evaluating changes in ECV from serial thoracic non-gated contrast CT scans in 32 female patients with breast cancer who had examination before chemotherapy and repeat examination after completion of anthracycline based chemotherapy regimen (ECV was derived from non-gated pre-contrast and delayed phase scans obtained at 7 min post contrast injection) (71). The authors found increased ECV values post therapy (30.0 ± 5.1%) when compared to pre-treatment ECV values (26.4 ± 3.8%).

The traditional contrast equilibrium method for ECV calculation has some potential technical challenges: (1) this approach requires both pre and post contrast scanning which despite the low dose nature of these scans, increases radiation dose, (2) difficulty in left ventricular segmentation of pre-contrast images, and (3) difficulty in the registration of the pre- and post-contrast images. However, dual source dual energy CT imaging offers a potential solution to these problems by performing a single scan with two orthogonally mounted detectors and tube arrays. This method can not only help with reducing beam hardening and metallic artifacts, but can potentially be

used for quantifying ECV with the potential of eliminating the requirement of pre-contrast images reducing problems with mis-registration as well as reducing radiation dose. Hong et al. evaluated ECV by dual energy CTA in a rabbit model of dilated cardiomyopathy, generated by administering 1.0 mg/kg of doxorubicin twice weekly for 16 weeks (69). The mean ECV values were significantly higher after doxorubicin administration (baseline: 28.5%, 6 weeks: 35.3%, 12 weeks: 41.9% and 16 weeks: 42.1%) (**Figure 5**). ECV obtained with dual energy CT correlated remarkably very well with ECV estimated by CMR and fibrosis extent on histology. Zhao et al. also compared the use of dual energy CT with single energy CT for the estimation of ECV in a canine model of doxorubicin induced cardiotoxicity (75). Dual energy CT ECV analysis was performed by using iodine maps generated from delayed CT images acquired at 100 and 140 kVp. As the authors hypothesized, the ECV CT index derived by dual energy CT correlated well with ECV estimated with single energy CT at 100 kVp and with histological analysis.

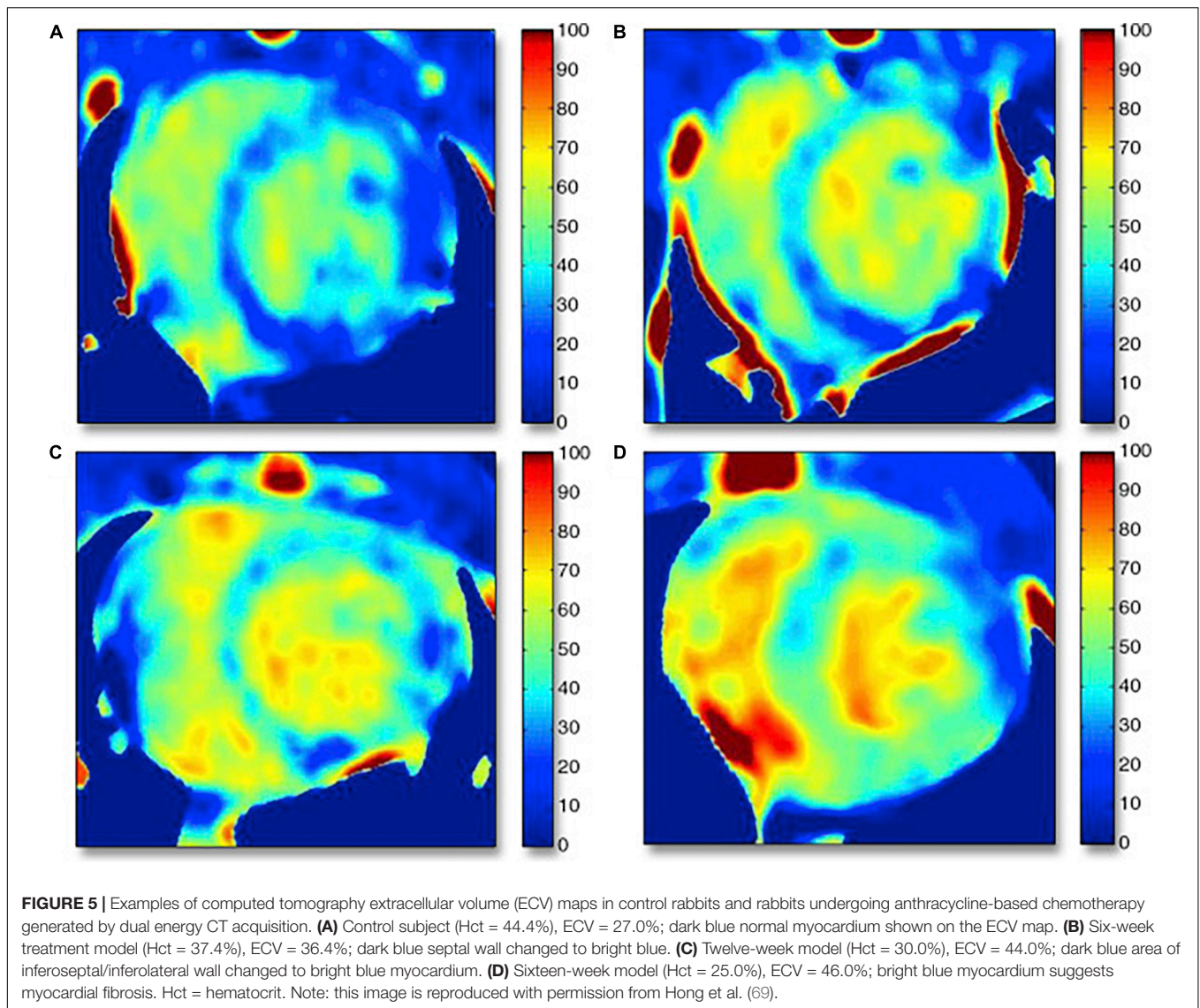## CT MOLECULAR IMAGING AND THERANOSTICS

Advancements in basic science and innovations in technology have led to a deeper understanding of the molecular and cellular processes that contribute to the pathophysiology of AIC. Molecular imaging, defined as the visualization, characterization, and non-invasive measurement of biological processes at the molecular and cellular level, has the ability to translate advancements in basic science to humans to facilitate early diagnosis, improve prognostication and guide targeted therapy across the spectrum of cardiovascular disease. Several molecular probes have been evaluated to interrogate molecular mechanisms which have been implicated in the pathophysiology of AIC by using predominantly radiolabeled imaging probes. The higher sensitivity of these radiolabeled probes makes nuclear imaging techniques more suitable for cardiac molecular imaging, however the wide availability of the clinical CT scanners and the fast scanning times coupled with high spatial resolution make CT a promising alternative approach for certain molecular imaging targets with high receptor density.

The currently used iodine-based contrast agents provide excellent tissue contrast for anatomic evaluation; however, these agents show rapid blood clearance and non-specific tissue distribution, both of which limit their use for targeted imaging. To overcome these issues, novel nanoparticles (1–100 nm diameter) have recently been assembled that incorporate high payloads of iodinated or inorganic contrast agents that may also use specific peptides or antibodies for improved sensitivity to detect molecular/cellular targets, while also improving signal-to-noise ratio (76). Moreover, theranostic platforms have also been designed that combine diagnostic properties with the capability of targeted delivery of therapies. As an example Zhu et al. constructed a unique theranostic platform for targeted chemotherapy and *in vitro* cancer cell imaging based on dendrimer-entrapped gold nanoparticles (CT contrast agent)

conjugated with doxorubicin (77). Similarly, Lin et al. developed a β-cyclodextrin based micelle system which was successfully loaded with gold nanoparticles and doxorubicin achieving high drug delivery and favorable imaging properties (78). In the future these and similar theranostic agents could be potentially used for pre-clinical investigations to further enhance our understanding of AIC. Nuclear molecular imaging techniques have already been successfully applied to track inflammation by detecting reactive oxygen species formation (12) and matrix metalloproteinase activity (23) in animal models of AIC. Imaging these processes by CT based molecular imaging probes, as well as CT based imaging of molecular processes involved in the pathophysiology of AIC, such as apoptosis, fibrosis and angiogenesis holds great promise for the future. Specifically, pre-clinical molecular imaging with CT has already been applied for the imaging of fibrosis by targeting collagen (79), or imaging inflammation by targeting E-selectin (80).

Nanoparticulate CT agents have been applied successfully in multiple preclinical models in a wide variety of cardiovascular diseases, however the full clinical potential of these probes will not be achieved until these barriers can be overcome, in particular the issue of sensitivity. Multiple liposomal formulations without imageable properties assembled for drug delivery have been successfully translated to clinical applications and used in early phase clinical trials for the delivery of anti-cancer, anti-fungal, anti-inflammatory drugs and for the delivery of therapeutic genes. The use of this nanoparticulate therapy provides local delivery of high therapeutic doses, potentially minimizing systemic toxicity, and this topic has been reviewed extensively (81). Several clinical trials have demonstrated favorable pharmacokinetic and pharmacodynamic profiles for these liposomal agents, along with excellent bioavailability and most importantly favorable safety profile in humans. An intravenously administered product named PEGylated liposomal iodixanol injection (NCTX), which has been previously tested in small and large animal models (82), has entered phase 1 tolerability and pharmacokinetic study in healthy volunteers (ClinicalTrials.gov identifier: NCT02063594).

The addition of nanoparticulate contrast agents containing inorganic contrast agents provide a unique opportunity for the visualization of a therapeutic agent, referred to as a theranostic. State-of-the-art clinical CT scanners already have the capability for acquiring the images with dual-energy by using either multiple layers of detectors or by employing rapid kilovolt switching from a single x-ray tube or different energy sources from dual source scanners (83). Visualization of materials is facilitated by the availability of modern clinical software equipped with capability for digital subtraction, effective anatomic number imaging and virtual monoenergetic reconstruction. Coupled with the use of novel inorganic agents these technologies can facilitate myocardial tissue characterization by allowing for material decomposition analysis. However, the human use inorganic contrast agents need to face some clinical challenges. Gold containing nanoparticles have been tested in clinical trials for cancer drug delivery demonstrating accumulation of gold

**FIGURE 5 |** Examples of computed tomography extracellular volume (ECV) maps in control rabbits and rabbits undergoing anthracycline-based chemotherapy generated by dual energy CT acquisition. **(A)** Control subject (Hct = 44.4%), ECV = 27.0%; dark blue normal myocardium shown on the ECV map. **(B)** Six-week treatment model (Hct = 37.4%), ECV = 36.4%; dark blue septal wall changed to bright blue. **(C)** Twelve-week model (Hct = 30.0%), ECV = 44.0%; dark blue area of inferoseptal/inferolateral wall changed to bright blue myocardium. **(D)** Sixteen-week model (Hct = 25.0%), ECV = 46.0%; bright blue myocardium suggests myocardial fibrosis. Hct = hematocrit. Note: this image is reproduced with permission from Hong et al. (69).

nanoparticles in the tumor tissue, but also considerable liver uptake after administration with only about 50% elimination at 120 day after treatment (84). Importantly *in vivo* imaging of nanoparticles was not attempted in these trials, and current concentrations of the gold may be insufficient for *in vivo* imaging. Therefore, while molecular imaging with CT is a promising new avenue, this theranostic approach is not yet ready for widespread clinical application.

## ROLE OF MULTIMODALITY IMAGING IN EVALUATION OF ANTHRACYCLINE-INDUCED CARDIOTOXICITY

Anthracycline toxicity can have an insidious presentation, and therefore early recognition of the underlying disease

process is very important to initiate preventive measures or to modify the anti-neoplastic therapeutic approach. In addition to the emerging role of CT, other imaging modalities can provide invaluable information about cardiac function that can help with management of AIC. Left ventricular ejection fraction (LVEF) assessment remains the key diagnostic parameter for the monitoring of anthracycline related cardiac dysfunction (85). Transthoracic echocardiography is the first line method for LVEF and strain evaluation (86), however cardiac MRI is emerging as the new gold standard of 3-dimensional quantification of global function and strain and has a growing role in the field (87). Equilibrium radionucleotide angiocardiography remains an accurate technique for LVEF assessment, although being used less frequently clinically for surveillance of cardiotoxicity due to concern of serial radiation exposure. In addition, the assessment of LVEF by CT and 3D echocardiography are newer alternatives for accurate assessment global function

as well as regional function. Growing literature supports the use of echocardiographic LV strain to identify sub-clinical left ventricular dysfunction in patients undergoing anthracycline-based chemotherapy (27). CT and MRI provide alternative methods for the accurate and reproducible assessment of regional myocardial deformation strain. Therefore, a multimodality imaging approach is recommended and often applied.

## CONCLUSION

Cardiac CT is a rapidly evolving technology for the evaluation of cardiac structures with or without contrast administration, including the evaluation of the underlying coronary anatomy and/or complicating atherosclerotic or thrombotic disease. With emerging new techniques, CT is rapidly evolving to provide information beyond the evaluation of epicardial coronary arteries including myocardial deformation assessment,

extracellular volume quantification, information about coronary vasoreactivity and even potential applications for molecular imaging. These new methodologies hold promise in the future for the early evaluation and management of AIC.

## AUTHOR CONTRIBUTIONS

AF drafted the manuscript. LB and AS reviewed and edited the manuscript. All authors contributed to the article and approved the submitted version.

## FUNDING

## REFERENCES

1. Siegel RL, Miller KD, Fuchs HE, Jemal A. Cancer Statistics, 2021. *CA Cancer J Clin.* (2021) 71:7–33.

2. Miller KD, Nogueira L, Mariotto AB, Rowland JH, Yabroff KR, Alfano CM, et al. Cancer treatment and survivorship statistics, 2019. *CA Cancer J Clin.* (2019) 69:363–85. doi: 10.3322/caac.21565

3. Minotti G, Menna P, Salvatorelli E, Cairo G, Gianni L. Anthracyclines: molecular advances and pharmacologic developments in antitumor activity and cardiotoxicity. *Pharmacol Rev.* (2004) 56:185–229. doi: 10.1124/pr.56.2.6

4. Dimarco A, Gaetani M, Orezzi P, Scarpinato BM, Silvestrini R, Soldati M, et al. 'Daunomycin', a New Antibiotic of the Rhodomycin Group. *Nature.* (1964) 201:706–7. doi: 10.1038/201706a0

5. Mcgowan JV, Chung R, Maulik A, Piotrowska I, Walker JM, Yellon DM. Anthracycline Chemotherapy and Cardiotoxicity. *Cardiovasc Drugs Ther.* (2017) 31:63–75.

6. Lefrak EA, Pitha J, Rosenheim S, Gottlieb JA. A clinicopathologic analysis of adriamycin cardiotoxicity. *Cancer.* (1973) 32:302–14. doi: 10.1002/1097-0142(197308)32:2&lt;302::aid-cncr2820320205&gt;3.0.co;2-2

7. Von Hoff DD, Layard MW, Basa P, Davis HL Jr., Von Hoff AL, Rozencweig M, et al. Risk factors for doxorubicin-induced congestive heart failure. *Ann Intern Med.* (1979) 91:710–7. doi: 10.7326/0003-4819-91-5-710

8. Swain SM, Whaley FS, Ewer MS. Congestive heart failure in patients treated with doxorubicin: a retrospective analysis of three trials. *Cancer.* (2003) 97:2869–79. doi: 10.1002/cncr.11407

9. Ewer MS, Ewer SM. Cardiotoxicity of anticancer treatments. *Nat Rev Cardiol.* (2015) 12:547–58. doi: 10.1038/nrcardio.2015.65

10. Myers CE, Mcguire WP, Liss RH, Ifrim I, Grotzinger K, Young RC. Adriamycin: the role of lipid peroxidation in cardiac toxicity and tumor response. *Science.* (1977) 197:165–7. doi: 10.1126/science.877547

11. Sarvazyan N. Visualization of doxorubicin-induced oxidative stress in isolated cardiac myocytes. *Am J Physiol.* (1996) 271:H2079–85. doi: 10.1152/ajpheart.1996.271.5.H2079

12. Boutagy NE, Wu J, Cai Z, Zhang W, Booth CJ, Kyriakides TC, et al. In Vivo Reactive Oxygen Species Detection With a Novel Positron Emission Tomography Tracer, (18)F-DHMT, Allows for Early Detection of Anthracycline-Induced Cardiotoxicity in Rodents. *JACC Basic Transl Sci.* (2018) 3:378–90. doi: 10.1016/j.jacbts.2018.02.003

13. Wu J, Boutagy NE, Cai Z, Lin SF, Zheng MQ, Feher A, et al. Feasibility study of PET dynamic imaging of [(18)F]DHMT for quantification of reactive oxygen species in the myocardium of large animals. *J Nucl Cardiol.* (2020) 29:216–25. doi: 10.1007/s12350-020-02184-3

14. Majzner K, Wojcik T, Szafraniec E, Lukawska M, Oszczapowicz I, Chlopicki S, et al. Nuclear accumulation of anthracyclines in the endothelium studied

by bimodal imaging: fluorescence and Raman microscopy. *Analyst.* (2015) 140:2302–10. doi: 10.1039/c4an01882f

15. Kotamraju S, Konorev EA, Joseph J, Kalyanaraman B. Doxorubicin-induced apoptosis in endothelial cells and cardiomyocytes is ameliorated by nitrone spin traps and ebselen. Role of reactive oxygen and nitrogen species. *J Biol Chem.* (2000) 275:33585–92. doi: 10.1074/jbc.M003890200

16. Monti M, Terzuoli E, Ziche M, Morbidelli L. The sulphydryl containing ACE inhibitor Zofenoprilat protects coronary endothelium from Doxorubicin-induced apoptosis. *Pharmacol Res.* (2013) 76:171–81. doi: 10.1016/j.phrs.2013.08.003

17. Vasquez-Vivar J, Martasek P, Hogg N, Masters BS, Pritchard KA Jr., Kalyanaraman B. Endothelial nitric oxide synthase-dependent superoxide generation from adriamycin. *Biochemistry.* (1997) 36:11293–7. doi: 10.1021/bi971475e

18. Sacco G, Mario B, Lopez G, Evangelista S, Manzini S, Maggi CA. ACE inhibition and protection from doxorubicin-induced cardiotoxicity in the rat. *Vascul Pharmacol.* (2009) 50:166–70. doi: 10.1016/j.vph.2009.01.001

19. Rasanen M, Degerman J, Nissinen TA, Miinalainen I, Kerkela R, Siltanen A, et al. VEGF-B gene therapy inhibits doxorubicin-induced cardiotoxicity by endothelial protection. *Proc Natl Acad Sci USA.* (2016) 113:13144–9. doi: 10.1073/pnas.1616168113

20. Luu AZ, Chowdhury B, Al-Omran M, Teoh H, Hess DA, Verma S. Role of Endothelium in Doxorubicin-Induced Cardiomyopathy. *JACC Basic Transl Sci.* (2018) 3:861–70. doi: 10.1016/j.jacbts.2018.06.005

21. Xue CB, Voss ME, Nelson DJ, Duan JJ, Cherney RJ, Jacobson IC, et al. Design, synthesis, and structure-activity relationships of macrocyclic hydroxamic acids that inhibit tumor necrosis factor alpha release in vitro and in vivo. *J Med Chem.* (2001) 44:2636–60. doi: 10.1021/jm010127e

22. Su H, Spinale FG, Dobrucki LW, Song J, Hua J, Sweterlitsch S, et al. Noninvasive targeted imaging of matrix metalloproteinase activation in a murine model of postinfarction remodeling. *Circulation.* (2005) 112:3157–67. doi: 10.1161/CIRCULATIONAHA.105.583021

23. Boutagy NE, Feher A, Pfau D, Liu Z, Guerrera NM, Freeburg LA, et al. Dual Angiotensin Receptor-Neprilysin Inhibition With Sacubitril/Valsartan Attenuates Systolic Dysfunction in Experimental Doxorubicin-Induced Cardiotoxicity. *JACC CardioOncol.* (2020) 2:774–87. doi: 10.1016/j.jaccao.2020.09.007

24. Lopez-Mattei JC, Yang EH, Ferencik M, Baldassarre LA, Dent S, Budoff MJ. Cardiac computed tomography in cardio-oncology: JACC: cardiooncology primer. *JACC CardioOncol.* (2021) 3:635–49. doi: 10.1016/j.jaccao.2021.09.010

25. Arnoldi E, Johnson TR, Rist C, Wintersperger BJ, Sommer WH, Becker A, et al. Adequate image quality with reduced radiation dose in prospectively triggered coronary CTA compared with retrospective techniques. *Eur Radiol.* (2009) 19:2147–55. doi: 10.1007/s00330-009-1411-9

26. Juergens KU, Grude M, Maintz D, Fallenberg EM, Wichter T, Heindel W, et al. Multi-detector row CT of left ventricular function with dedicated analysis software versus MR imaging: initial experience. *Radiology*. (2004) 230:403–10. doi: 10.1148/radiol.2302030042

27. Oikonomou EK, Kokkinidis DG, Kampaktsis PN, Amir EA, Marwick TH, Gupta D, et al. Assessment of prognostic value of left ventricular global longitudinal strain for early prediction of chemotherapy-induced cardiotoxicity: a systematic review and meta-analysis. *JAMA Cardiol*. (2019) 4:1007–18. doi: 10.1001/jamacardio.2019.2952

28. Feher A, Boutagy NE, Stendahl JC, Hawley C, Guerrera N, Booth CJ, et al. Computed Tomographic Angiography Assessment of Epicardial Coronary Vasoreactivity for Early Detection of Doxorubicin-Induced Cardiotoxicity. *JACC CardioOncol*. (2020) 2:207–19. doi: 10.1016/j.jaccao.2020.05.007

29. Thavendiranathan P, Negishi T, Somerset E, Negishi K, Penicka M, Lemieux J, et al. Strain-Guided Management of Potentially Cardiotoxic Cancer Therapy. *J Am Coll Cardiol*. (2021) 77:392–401.

30. Shi P, Sinusas AJ, Constable RT, Ritman E, Duncan JS. Point-tracked quantitative analysis of left ventricular surface motion from 3-D image sequences. *IEEE Trans Med Imaging*. (2000) 19:36–50. doi: 10.1109/42.832958

31. Pourmorteza A, Schuleri KH, Herzka DA, Lardo AC, Mcveigh ER. A new method for cardiac computed tomography regional function assessment: stretch quantifier for endocardial engraved zones (SQUEEZ). *Circ Cardiovasc Imaging*. (2012) 5:243–50. doi: 10.1161/CIRCIMAGING.111.970061

32. Tee MW, Won S, Raman FS, Yi C, Vigneault DM, Davies-Venn C, et al. Regional Strain Analysis with Multidetector CT in a Swine Cardiomyopathy Model: Relationship to Cardiac MR Tagging and Myocardial Fibrosis. *Radiology*. (2015) 277:88–94. doi: 10.1148/radiol.2015142339

33. Midgett DE, Thorn SL, Ahn SS, Uman S, Avendano R, Melvinsdottir I, et al. CineCT platform for in vivo and ex vivo measurement of 3D high resolution Lagrangian strains in the left ventricle following myocardial infarction and intramyocardial delivery of theranostic hydrogel. *J Mol Cell Cardiol*. (2022) 166:74–90. doi: 10.1016/j.yjmcc.2022.02.004

34. Marwan M, Ammon F, Bittner D, Rother J, Mekkhala N, Hell M, et al. CT-derived left ventricular global strain in aortic valve stenosis patients: a comparative analysis pre and post transcatheter aortic valve implantation. *J Cardiovasc Comput Tomogr*. (2018) 12:240–4. doi: 10.1016/j.jcct.2018.01.010

35. Ammon F, Bittner D, Hell M, Mansour H, Achenbach S, Arnold M, et al. CT-derived left ventricular global strain: a head-to-head comparison with speckle tracking echocardiography. *Int J Cardiovasc Imaging*. (2019) 35:1701–7. doi: 10.1007/s10554-019-01596-8

36. Fukui M, Xu J, Thoma F, Sultan I, Mulukutla S, Elzomor H, et al. Baseline global longitudinal strain by computed tomography is associated with post transcatheter aortic valve replacement outcomes. *J Cardiovasc Comput Tomogr*. (2020) 14:233–9. doi: 10.1016/j.jcct.2019.12.002

37. Peled Z, Lamash Y, Carasso S, Fischer A, Agmon Y, Mutlak D, et al. Automated 4-dimensional regional myocardial strain evaluation using cardiac computed tomography. *Int J Cardiovasc Imaging*. (2020) 36:149–59. doi: 10.1007/s10554-019-01696-5

38. Wang R, Fang Z, Wang H, Schoepf UJ, Emrich T, Giovagnoli D, et al. Quantitative analysis of three-dimensional left ventricular global strain using coronary computed tomography angiography in patients with heart failure: comparison with 3T cardiac MR. *Eur J Radiol*. (2021) 135:109485. doi: 10.1016/j.ejrad.2020.109485

39. Lu A, Ahn SS, Ta K, Parajuli N, Stendahl JC, Liu Z, et al. Learning-Based Regularization for Cardiac Strain Analysis via Domain Adaptation. *IEEE Trans Med Imaging*. (2021) 40:2233–45. doi: 10.1109/TMI.2021.3074033

40. Guo Y, Bi L, Zhu Z, Feng DD, Zhang R, Wang Q, et al. Automatic left ventricular cavity segmentation via deep spatial sequential network in 4D computed tomography. *Comput Med Imaging Graph*. (2021) 91:101952. doi: 10.1016/j.compmedimag.2021.101952

41. Vach M, Vogelhuber J, Weber M, Sprinkart AM, Pieper CC, Block W, et al. Feasibility of CT-derived myocardial strain measurement in patients with advanced cardiac valve disease. *Sci Rep*. (2021) 11:8793. doi: 10.1038/s41598-021-88294-5

42. Gulati M, Levy PD, Mukherjee D, Amsterdam E, Bhatt DL, Birtcher KK, et al. 2021 AHA/ACC/ASE/CHEST/SAEM/SCCT/SCMR guideline for the evaluation and diagnosis of chest pain: a report of the american college of cardiology/american heart association joint committee on clinical practice guidelines. *Circulation*. (2021) 144:e368–454.

43. Pinder MC, Duan Z, Goodwin JS, Hortobagyi GN, Giordano SH. Congestive heart failure in older women treated with adjuvant anthracycline chemotherapy for breast cancer. *J Clin Oncol*. (2007) 25:3808–15. doi: 10.1200/JCO.2006.10.4976

44. Bozkurt B, Hershberger RE, Butler J, Grady KL, Heidenreich PA, Isler ML, et al. 2021 ACC/AHA key data elements and definitions for heart failure: a report of the american college of cardiology/american heart association task force on clinical data standards (writing committee to develop clinical data standards for heart failure). *Circ Cardiovasc Qual Outcomes*. (2021) 14:e000102.

45. Andreini D, Pontone G, Pepi M, Ballerini G, Bartorelli AL, Magini A, et al. Diagnostic accuracy of multidetector computed tomography coronary angiography in patients with dilated cardiomyopathy. *J Am Coll Cardiol*. (2007) 49:2044–50. doi: 10.1016/j.jacc.2007.01.086

46. Bhatti S, Hakeem A, Yousuf MA, Al-Khalidi HR, Mazur W, Shizukuda Y. Diagnostic performance of computed tomography angiography for differentiating ischemic vs nonischemic cardiomyopathy. *J Nucl Cardiol*. (2011) 18:407–20. doi: 10.1007/s12350-011-9346-3

47. Daher IN, Banchs J, Yusuf SW, Mouhayar E, Durand JB, Gladish G. Impact of cardiac computed tomographic angiography findings on planning of cancer therapy in patients with concomitant structural heart disease. *Cardiol Res Pract*. (2011) 2011:268058. doi: 10.4061/2011/268058

48. Cardinale D, Sandri MT, Colombo A, Colombo N, Boeri M, Lamantia G, et al. Prognostic value of troponin in cardiac risk stratification of cancer patients undergoing high-dose chemotherapy. *Circulation*. (2004) 109:2749–54. doi: 10.1161/01.CIR.0000130926.51766.CC

49. Antoniak S, Phungphong S, Cheng Z, Jensen BC. Novel mechanisms of anthracycline-induced cardiovascular toxicity: a focus on thrombosis, cardiac atrophy, and programmed cell death. *Front Cardiovasc Med*. (2021) 8:817977. doi: 10.3389/fcvm.2021.817977

50. Kelkar AA, Schultz WM, Khosa F, Schulman-Marcus J, O'hartaigh BW, Gransar H, et al. Long-Term Prognosis After Coronary Artery Calcium Scoring Among Low-Intermediate Risk Women and Men. *Circ Cardiovasc Imaging*. (2016) 9:e003742. doi: 10.1161/CIRCIMAGING.115.003742

51. Lehmann N, Erbel R, Mahabadi AA, Rauwolf M, Mohlenkamp S, Moebus S, et al. value of progression of coronary artery calcification for risk prediction of coronary and cardiovascular events: result of the HNR study (Heinz Nixdorf Recall). *Circulation*. (2018) 137:665–79. doi: 10.1161/CIRCULATIONAHA.116.027034

52. Takx RA, De Jong PA, Leiner T, Oudkerk M, De Koning HJ, Mol CP, et al. Automated coronary artery calcification scoring in non-gated chest CT: agreement and reliability. *PLoS One*. (2014) 9:e91239. doi: 10.1371/journal.pone.0091239

53. El-Sabbagh A, Osman MM, Fesler M, Helmy T, Parker N, Muzaffar R. Chemotherapy-induced coronary arteries calcium score deterioration as detected with unenhanced CT portion of FDG PET/CT. *Am J Nucl Med Mol Imaging*. (2018) 8:303–10.

54. Hecht HS, Cronin P, Blaha MJ, Budoff MJ, Kazerooni EA, Narula J, et al. 2016 SCCT/STR guidelines for coronary artery calcium scoring of noncontrast noncardiac chest CT scans: a report of the Society of Cardiovascular Computed Tomography and Society of Thoracic Radiology. *J Cardiovasc Comput Tomogr*. (2017) 11:74–84. doi: 10.1016/j.jcct.2016.11.003

55. Kim RJ, Wu E, Rafael A, Chen EL, Parker MA, Simonetti O, et al. The use of contrast-enhanced magnetic resonance imaging to identify reversible myocardial dysfunction. *N Engl J Med*. (2000) 343:1445–53. doi: 10.1056/NEJM200011163432003

56. Gulati A, Jabbour A, Ismail TF, Guha K, Khwaja J, Raza S, et al. Association of fibrosis with mortality and sudden cardiac death in patients with nonischemic dilated cardiomyopathy. *JAMA*. (2013) 309:896–908. doi: 10.1001/jama.2013.1363

57. Kuruvilla S, Adenaw N, Katwal AB, Lipinski MJ, Kramer CM, Salerno M. Late gadolinium enhancement on cardiac magnetic resonance predicts adverse cardiovascular outcomes in nonischemic cardiomyopathy: a systematic review and meta-analysis. *Circ Cardiovasc Imaging*. (2014) 7:250–8. doi: 10.1161/CIRCIMAGING.113.001144

58. Dang Y, Hou Y. The prognostic value of late gadolinium enhancement in heart diseases: an umbrella review of meta-analyses of observational studies. *Eur Radiol.* (2021) 31:4528–37. doi: 10.1007/s00330-020-07437-w

59. Diao KY, Yang ZG, Xu HY, Liu X, Zhang Q, Shi K, et al. Histologic validation of myocardial fibrosis measured by T1 mapping: a systematic review and meta-analysis. *J Cardiovasc Magn Reson.* (2016) 18:92. doi: 10.1186/s12968-016-0313-7

60. Kammerlander AA, Marzluf BA, Zotter-Tufaro C, Aschauer S, Duca F, Bachmann A, et al. T1 mapping by CMR imaging: from histological validation to clinical implication. *JACC Cardiovasc Imaging.* (2016) 9:14–23. doi: 10.1016/j.jcmg.2015.11.002

61. Nakamori S, Dohi K, Ishida M, Goto Y, Imanaka-Yoshida K, Omori T, et al. Native T1 Mapping and Extracellular Volume Mapping for the Assessment of Diffuse Myocardial Fibrosis in Dilated Cardiomyopathy. *JACC Cardiovasc Imaging.* (2018) 11:48–59. doi: 10.1016/j.jcmg.2017.04.006

62. Neilan TG, Coelho-Filho OR, Shah RV, Feng JH, Pena-Herrera D, Mandry D, et al. Myocardial extracellular volume by cardiac magnetic resonance imaging in patients treated with anthracycline-based chemotherapy. *Am J Cardiol.* (2013) 111:717–22. doi: 10.1016/j.amjcard.2012.11.022

63. Jordan JH, Vasu S, Morgan TM, D'agostino RB Jr., Melendez GC, Hamilton CA, et al. Anthracycline-Associated T1 Mapping Characteristics Are Elevated Independent of the Presence of Cardiovascular Comorbidities in Cancer Survivors. *Circ Cardiovasc Imaging.* (2016) 9:e004325. doi: 10.1161/CIRCIMAGING.115.004325

64. Ferreira De Souza T, Quinaglia ACST, Osorio Costa F, Shah R, Neilan TG, et al. Anthracycline Therapy Is Associated With Cardiomyocyte Atrophy and Preclinical Manifestations of Heart Disease. *JACC Cardiovasc Imaging.* (2018) 11:1045–55. doi: 10.1016/j.jcmg.2018.05.012

65. Nacif MS, Kawel N, Lee JJ, Chen X, Yao J, Zavodni A, et al. Interstitial myocardial fibrosis assessed as extracellular volume fraction with low-radiation-dose cardiac CT. *Radiology.* (2012) 264:876–83. doi: 10.1148/radiol.12112458

66. Bandula S, White SK, Flett AS, Lawrence D, Pugliese F, Ashworth MT, et al. Measurement of myocardial extracellular volume fraction by using equilibrium contrast-enhanced CT: validation against histologic findings. *Radiology.* (2013) 269:396–403. doi: 10.1148/radiology.13130130

67. Lee HJ, Im DJ, Youn JC, Chang S, Suh YJ, Hong YJ, et al. Myocardial extracellular volume fraction with dual-energy equilibrium contrast-enhanced cardiac CT in nonischemic cardiomyopathy: a prospective comparison with cardiac MR imaging. *Radiology.* (2016) 280:49–57. doi: 10.1148/radiol.2016151289

68. Suzuki M, Toba T, Izawa Y, Fujita H, Miwa K, Takahashi Y, et al. Prognostic Impact of Myocardial Extracellular Volume Fraction Assessment Using Dual-Energy Computed Tomography in Patients Treated With Aortic Valve Replacement for Severe Aortic Stenosis. *J Am Heart Assoc.* (2021) 10:e020655. doi: 10.1161/JAHA.120.020655

69. Hong YJ, Kim TK, Hong D, Park CH, Yoo SJ, Wickum ME, et al. Myocardial Characterization Using Dual-Energy CT in Doxorubicin-Induced DCM: comparison With CMR T1-Mapping and Histology in a Rabbit Model. *JACC Cardiovasc Imaging.* (2016) 9:836–45. doi: 10.1016/j.jcmg.2015.12.018

70. Zhou Z, Xu L, Wang R, Varga-Szemes A, Durden JA, Joseph Schoepf U, et al. Quantification of doxorubicin-induced interstitial myocardial fibrosis in a beagle model using equilibrium contrast-enhanced computed tomography: a comparative study with cardiac magnetic resonance T1-mapping. *Int J Cardiol.* (2019) 281:150–5. doi: 10.1016/j.ijcard.2019.01.021

71. Monti CB, Zanardo M, Bosetti T, Ali M, De Benedictis E, Luporini A, et al. Assessment of myocardial extracellular volume on body computed tomography in breast cancer patients treated with anthracyclines. *Quant Imaging Med Surg.* (2020) 10:934–44. doi: 10.21037/qims.2020.04.05

72. Sueta D, Kidoh M, Oda S, Tsujita K. Novel assessment of cancer therapy-related cardiac dysfunction by cardiac computed tomography: a case report. *Eur Heart J Case Rep.* (2020) 4:1–2. doi: 10.1093/ehjcr/ytaa246

73. Egashira K, Sueta D, Tomiguchi M, Kidoh M, Oda S, Usuku H, et al. Cardiac computed tomography-derived extracellular volume fraction in late anthracycline-induced cardiotoxicity. *Int J Cardiol Heart Vasc.* (2021) 34:100797. doi: 10.1016/j.ijcha.2021.100797

74. Sueta D, Kidoh M, Oda S, Egashira K, Yamamoto E, Kaikita K, et al. Usefulness of Cardiac Computed Tomography in the Diagnosis of Anti-Cancer Therapy-Related Cardiac Dysfunction- Consistency With Magnetic Resonance Imaging. *Circ J.* (2021) 85:393–6. doi: 10.1253/circj.CJ-20-1288

75. Zhou Z, Gao Y, Wang H, Wang W, Zhang H, Wang S, et al. Myocardial extracellular volume fraction analysis in doxorubicin-induced beagle models: comparison of dual-energy CT with equilibrium contrast-enhanced single-energy CT. *Cardiovasc Diagn Ther.* (2021) 11:102–10. doi: 10.21037/cdt-20-798

76. Hyafil F, Cornily JC, Feig JE, Gordon R, Vucic E, Amirbekian V, et al. Noninvasive detection of macrophages using a nanoparticulate contrast agent for computed tomography. *Nat Med.* (2007) 13:636–41. doi: 10.1038/nm1571

77. Zhu J, Wang G, Alves CS, Tomas H, Xiong Z, Shen M, et al. Multifunctional Dendrimer-Entrapped Gold Nanoparticles Conjugated with Doxorubicin for pH-Responsive Drug Delivery and Targeted Computed Tomography Imaging. *Langmuir.* (2018) 34:12428–35. doi: 10.1021/acs.langmuir.8b02901

78. Lin W, Zhang X, Qian L, Yao N, Pan Y, Zhang L. Doxorubicin-Loaded Unimolecular Micelle-Stabilized Gold Nanoparticles as a Theranostic Nanoplatform for Tumor-Targeted Chemotherapy and Computed Tomography Imaging. *Biomacromolecules.* (2017) 18:3869–80. doi: 10.1021/acs.biomac.7b00810

79. Danila D, Johnson E, Kee P. CT imaging of myocardial scars with collagen-targeting gold nanoparticles. *Nanomedicine.* (2013) 9:1067–76. doi: 10.1016/j.nano.2013.03.009

80. Wyss C, Schaefer SC, Juillerat-Jeanneret L, Lagopoulos L, Lehr HA, Becker CD, et al. Molecular imaging by micro-CT: specific E-selectin imaging. *Eur Radiol.* (2009) 19:2487–94. doi: 10.1007/s00330-009-1434-2

81. Bulbake U, Doppalapudi S, Kommineni N, Khan W. Liposomal formulations in clinical use: an updated review. *Pharmaceutics.* (2017) 9:12. doi: 10.3390/pharmaceutics9020012

82. Izri MA, Belazzoug S, Pratlong F, Rioux JA. [Isolation of Leishmania major in Phlebotomus papatasi in Biskra (Algeria). The end of an ecoepidemiological saga]. *Ann Parasitol Hum Comp.* (1992) 67:31–2. doi: 10.1051/parasite/199267131

83. Nicol ED, Norgaard BL, Blanke P, Ahmadi A, Weir-Mccall J, Horvat PM, et al. The future of cardiovascular computed tomography: advanced analytics and clinical insights. *JACC Cardiovasc Imaging.* (2019) 12:1058–72. doi: 10.1016/j.jcmg.2018.11.037

84. Libutti SK, Paciotti GF, Byrnes AA, Alexander HR Jr., Gannon WE, Walker M, et al. Phase I and pharmacokinetic studies of CYT-6091, a novel PEGylated colloidal gold-rhTNF nanomedicine. *Clin Cancer Res.* (2010) 16:6139–49. doi: 10.1158/1078-0432.CCR-10-0978

85. Soufer A, Liu C, Henry ML, Baldassarre LA. Nuclear cardiology in the context of multimodality imaging to detect cardiac toxicity from cancer therapeutics: established and emerging methods. *J Nucl Cardiol.* (2020) 27:1210–24. doi: 10.1007/s12350-019-01671-6

86. Plana JC, Galderisi M, Barac A, Ewer MS, Ky B, Scherrer-Crosbie M, et al. Expert consensus for multimodality imaging evaluation of adult patients during and after cancer therapy: a report from the American Society of Echocardiography and the European Association of Cardiovascular Imaging. *J Am Soc Echocardiogr.* (2014) 27:911–39. doi: 10.1016/j.echo.2014.07.012

87. Kammerlander AA. Feature tracking by cardiovascular magnetic resonance imaging: the new gold standard for systolic function? *JACC Cardiovasc Imaging.* (2020) 13:948–50. doi: 10.1016/j.jcmg.2019.11.015